Integrative clinicopathological and molecular analyses of angioimmunoblastic T-cell lymphoma and other nodal lymphomas of follicular helper T-cell origin

Maria Pamela Dobay,[1] Francois Lemonnier,[2,3] Edoardo Missiaglia,[1,4] Christian Bastard,[5] David Vallois,[4] Jean-Philippe Jais,[6] Laurianne Scourzic,[7] Aurélie Dupuy,[2,3] Virginie Fataccioli,[2,3,14] Anais Pujals,[2,3,14] Marie Parrens,[8] Fabien Le Bras,[9] Thérèse Rousset,[10] Jean-Michel Picquenot,[11] Nadine Martin,[2,3] Corinne Haioun,[2,3,9] Richard Delarue,[12] Olivier A. Bernard,[7] Mauro Delorenzi,[1,13] Laurence de Leval[4] and Philippe Gaulard[2,3,14]**

[1]SIB Swiss Institute of Bioinformatics, Lausanne, Switzerland; [2]INSERM U955, Créteil, France; [3]Université Paris-Est, Créteil, France; [4]Institut de Pathologie, Centre Hospitalier Universitaire Vaudois, Lausanne, Switzerland; [5]Laboratoire de cytogénétique et biologie moléculaire, CLCC H.Becquerel, Rouen, France; [6]Service de Biostatistiques, GH Necker Enfants Malades, Paris, France; [7]Institute Gustave Roussy, Villejuif, France; [8]Departement de Pathologie, CHU de Bordeaux, Hopital du Haut Lévêque, Pessac, France; [9]Unité Hémopathies lymphoïdes, Hôpital Henri Mondor, AP-HP, Créteil, France; [10]Service d'anatomo-pathologie, CHU Gui de Chauliac, Montpellier, France; [11]Service d'anatomo-pathologie, CLCC H. Becquerel, Rouen, France; [12]Hématologie Clinique, GH Necker-Enfants malades, Paris, France; [13]Ludwig Center for Cancer Research, University of Lausanne, Switzerland and [14]Hôpital Henri Mondor, Département de Pathologie, AP-HP, Créteil, France

**equal contributions*

Correspondence: philippe.gaulard@aphp.fr/ Laurence.deLeval@chuv.ch
doi:10.3324/haematol.2016.158428

Supplementary information

Supplemental Materials and Methods

Samples and data availability. All samples in the TENOMIC biobank were collected with the approval of the ethical committee CPP Ile-de-France 08-009 (1). Gene expression data and mutation data, in the form of variant call files (VCF), are available upon request.

Case review. AITL were defined using the classical morphological definition, including constellation of features comprising increased vascularity, follicular dendritic cell proliferation. PTCL-NOS was systematically applied to cases not expected to show a TFH phenotype, that is cytotoxic lymphomas and lymphomas strongly positive for CD30 (>50%). For other PTCLs, assignment to "NOS" category was for those not showing a TFH immunophenotype. For PTCL-NOS cases, cytological features determined based on the proportion of small, medium and large cells, were collapsed to two categories based on the predominance of the small or large cell component (2). All cases included in the study were of nodal origin.

Immunohistochemistry (IHC) and in-situ Hybridization studies

IHC analysis was performed as previously described (3). Briefly, follicular helper T-cell (TFH) markers (PD1, CXCL13, BCL6 and CD10) and cytotoxic markers were assigned based on the following scoring system: score 0: <10% positive tumour cells, score 1: 10-30% positive tumor cells, score 2: >30-50% positive tumor cells, score 3: >50% positive tumor cells. FDC distribution was evaluated by CD21 and/or CD23 immunostains and was assigned a score of 0 when signal is restricted to germinal centers (GC); 1 in case of perifollicular expansion; 2 in case of perifollicular and perivascular expansion; or 3 for diffuse expansion.

PTCL-NOS cases were scored for CD30 as previously described: 0: <5% positive tumour cells, score 1: 5-25% positive tumor cells, score 2: >25-50% positive tumor cells, score 3: >50-75% positive tumor cells and score 4: >75% positive tumor cells (2).

The EBV status in large lymphoid cells was based on counting EBER-positive large cells and scored as follows: score 0: absence of large EBV-positive cells; score 1: up to 5 large EBV-positive cells per high power field (hpf), score 2: 5 to 50 per hpf and score 3 : > 50 per hpf , or sheets or aggregates of large EBV-positive cells. A score of 1 was considered positive (+), and scores of 2 or 3 were considered strongly positive. FISH testing using a double fusion assay for detection of *ITK-SYK* fusion was successfully performed on nine AITL, five TFH-like PTCL, five F-PTCL and four PTCL-NOS cases according to a previously-described method (3).

Software. Unless otherwise specified, all computation was performed using R version 3.2.2.

OMICs data. Gene expression profiling was performed on Affymetrix HG-U133 plus 2.0 chips (Affymetrix, Santa Clara, CA) for 83 AITL, 21 TFH-PTCL, and 36 PTCL-NOS, as described in (4). Briefly, 3 ug total RNA and 10 ug cRNA were used as starting material per hybridization. The cRNAs were hybridized to HG-U133 plus 2.0 Affymetrix GeneChip arrays (Affymetrix, Santa Clara, CA) and scanned with an Affymetrix GeneChip Scanner 3000. Images were analyzed using GCOS 1.4 *Affymetrix). Data were normalized using the robust multiarray average (RMA) method. Array comparative genomic Hybridization (aCGH, Agilent SurePrint G3 human CGH bundle, 4 x180K, Santa Clara, CA) was available for 60 AITL, 15 TFH-PTCL and 27 PTCL-NOS.

Targeted Deep Sequencing. *TET2, IDH2* and *DNMT3A* mutation information (Sequenom MassARRAY, confirmed by Sanger sequencing) was available for 64 (*TET2, DNMT3A*) to 66

AITL (*IDH2*), up to 21 TFH-PTCL, and up to 24 PTCL-NOS. *TET2* mutation data for 56/64 AITLs and for 17/21 TFH-PTCL and 22/24 PTCL-NOS have been reported previously in Lemonnier et al. (5) *RHOA* G17V mutation information was available for 72 AITL and 42 PTCLs, including 19 TFH-PTCLs and 23 PTCL-NOS (MiSeq, Illumina, confirmed on PGM, Lifetechnologies). Of the 114 cases with *RHOA* mutation information, the status of 72/72 AITLs and 13/19 TFH PTCL cases have been previously reported in Vallois et al. (6).

Consensus Clustering. In order to evaluate the stability of F-PTCL clustering with either AITL or PTCL-NOS, we used a resampling-based method, Consensus Clustering (R package ConsensusClusterPlus, version 1.24.0)(7). Briefly, this method takes a random subset of the data (80% of the cohort) for each of 1000 runs and performs agglomerative hierarchical clustering. F-PTCL clustering with AITL or PTCL-NOS was scored for each run.

Gene set enrichment analysis (GSEA). Relevant signatures from the Molecular Signatures Database (8) (MSigDB), the lymphoid signature collection (9) (n = 271, http://lymphochip.nih.gov/signaturedb/), and TFH- and AITL-associated signatures from literature (4) (n=3), combined with a subset of relevant hallmark (n=50), immunological (n=6) and curated (n=73) signatures from MSigDB were selected for use in enrichment analysis. The TFH signature is a subset of the Chtanova TFH signature (10) that was previously reported to be enriched in AITL (4). The AITL signatures were comprised of a tumor signature, which are genes differentially expressed in AITL compared to PTCL-NOS; while the microenvironment signature was comprised of genes more highly expressed in the AITL tissue than in the FACS-sorted component (4). GSEA was performed by rotation testing using mean ranks (ROMER, R package limma, version 3.24.15) with multi-testing

correction (Benjamini-Hochberg) to control for false negatives. Gene set expression levels are expressed as the median value of all genes in a signature per sample.

Copy number analysis. Array comparative genomic hybridization profiles were available for 106 cases. Briefly, images of the arrays were obtained using the Axon 4000B scanner 1a and analyzed by Genepix 5.1 software (Axon, Union city, USA). The signals were log transformed and normalized by robust locally weighted regression and scaled using median absolute deviation (R package marray, version 1.46.0). Data were filtered in order to remove controls or spots with signal intensity below the 25% quantile in both channels. Data was smoothed to remove single point outliers before applying a circular binary segmentation algorithm, which tests the significance of the alteration by using a hybrid approach (R packages DNAcopy, version 1.42.0; cghMCR, version 1.26.0 (11)). Given the highly variable tumor content in PTCLs, especially of AITL, event calls were made individually for samples. Briefly, the aCGH segemented profile was scanned for *TCR* (alpha and delta subunits) rearrangements (chromosome 14q11-12). The absolute value of the signal at this region is considered the baseline for an event call (i.e. if the 14q11-12 signal for a sample A is at -0.1 and for sample B -0.2, then $|signals| \geq 0.1$ and $|signals| \geq 0.2$ will be considered events in samples A and B, respectively), rather than using a fixed threshold (typically 0.3). All differences in copy number variation were compared across pathological categories using Fisher's exact test.

Supplementary Table S1. Comparison of IHC scores for TFH markers and AITL features in AITL and TFH-PTCL

	AITL	TFH-like PTCL	F-PTCL	p-value across three categories	p-value, AITL vs. TFH-like
	Positive/Total* cases				
TFH markers					
CD10	65/73 (89%)	6/16 (38%)	4/5 (80%)	0.22	0.11
PD1	52/52 (100%)	8/10 (80%)	5/5 (100%)	0.95	0.8
CXCL13	49/51 (96%)	11/15 (73%)	5/5 (100%)	0.84	0.66
BCL6	50/55 (91%)	9/13 (69%)	4/4 (100%)	0.81	0.64
ICOS	45/46 (98%)	14/15 (93%)	4/4 (100%)	1	1
AITL features					
FDC	65/68 (95%)	7/16 (44%)	0/5 (0%)	*0.03*	0.12
B-blasts	70/71 (99%)	11/16 (69%)	4/5 (80%)	0.73	0.41
EBER	63/69 (91%)	13/16 (81%)	5/5 (100%)	0.96	0.84
	Strongly Positive/All Positive**				
TFH markers					
CD10	26/65 (40%)	3/6 (50%)	3/4 (75%)	0.62	0.72
PD1	46/52 (88%)	6/8 (75%)	5/5 (100%)	1	1
CXCL13	36/49 (73%)	7/11 (64%)	4/5 (80%)	1	1
BCL6	29/50 (58%)	5/9 (56%)	2/4 (50%)	1	1
ICOS	42/45 (93%)	12/14 (86%)	4/4 (100%)	1	1
AITL features					
FDC	52/65 (80%)	3/7 (43%)	0/0 (0%)	0.51	0.51
B-blasts	56/70 (80%)	5/11 (45%)	1/4 (25%)	0.38	0.42
EBER	30/63 (48%)	3/14 (21%)	2/5 (40%)	0.47	0.27

*Total cases do not include non-interpretable cases

** Strongly positive cases have a score of 2 or 3

Supplementary Table S2. Correlation coefficients of IHC scores and mRNA expression levels for TFH markers

Marker	Spearman correlation coefficient	p-value
BCL6	0.46	0.04
CXCL13	0.46	0.03
ICOS	0.16	0.47
MME (CD10)	0.57	0.004
PDCD1 (PD1)	0.39	0.12

Supplementary Table S3. Top 50 genes correlating with TFH status*

	Nodal lymphomas of TFH origin						
		Other TFH-PTCL					
Gene	AITL	TFH-like PTCL	F-PTCL	PTCL-NOS	Spearman correlation coefficient**	Adj. p-value	Pathway(s)
CD200	8.59	8.95	9.15	7.11	0.68	2.20E-16	TFH signature; AITL microenvironment signature
C4orf7	10.98	11.87	11.98	8.34	0.66	2.20E-16	
SPIB	7.22	7.91	8.2	6.23	0.65	2.20E-16	AITL microenvironment signature
POU2AF1	9.21	10.05	9.89	7.39	0.65	2.20E-16	TFH signature; AITL microenvironment signature
CLU	11.24	11.83	12.02	9.91	0.64	2.20E-16	AITL microenvironment signature
CXCL13	11.69	12.42	12.37	10.17	0.63	2.20E-16	TFH signature; AITL tumor signature
ADRA2A	7.47	7.95	8.43	6.11	0.63	2.20E-16	AITL microenvironment signature
EFNB2	7.09	7.71	7.58	6.31	0.62	5.58E-15	AITL microenvironment signature
ITIH5	6.18	6.74	6.52	5.37	0.62	5.58E-15	IL2 STAT5 Signaling; AITL microenvironment signature
PAPSS2	8.41	8.84	8.85	7.76	0.61	7.53E-15	AITL microenvironment signature
XKR4	5.09	5.89	5.93	3.87	0.61	9.12E-15	AITL microenvironment signature
CDC42EP4	6.14	6.69	6.88	5.62	0.61	1.25E-14	
PDIA5	7.12	7.57	7.25	6.56	0.59	8.49E-14	AITL microenvironment signature
GNA14	5.86	6.41	6.13	4.94	0.59	1.08E-13	AITL microenvironment signature
FAM171A1	6.62	7.09	7.15	5.96	0.59	1.08E-13	AITL microenvironment signature
TMEM163	7.68	8.09	8.11	6.53	0.59	1.08E-13	AITL microenvironment signature
COL4A4	6.6	7.33	6.95	5.68	0.58	4.10E-13	AITL microenvironment signature
ARHGEF10	6.81	7.26	7.36	6.13	0.58	5.73E-13	AITL microenvironment signature
P2RX5	8.81	8.91	9.22	7.62	0.58	5.78E-13	
CXCR5	7.01	7.07	8.05	5.46	0.57	9.18E-13	TFH signature
CHN1	8.58	9	9.15	7.76	0.56	2.35E-12	AITL microenvironment signature
SLC1A2	5.42	5.99	6.17	4.49	0.56	4.59E-12	AITL microenvironment signature

GJA4	6.04	6.5	6.25	5.61	0.56	4.90E-12	AITL microenvironment signature
LOC100507421	5.71	6.11	6.43	5.05	0.55	6.80E-12	
PDLIM1	9.44	9.8	9.82	8.84	0.55	7.36E-12	AITL microenvironment signature
IGHM	7.75	8.77	8.2	5.77	0.55	8.39E-12	
BTLA	7.88	7.86	8.05	6.21	0.55	8.39E-12	TFH signature
MOXD1	6.06	6.35	6.33	5.18	0.55	9.34E-12	AITL microenvironment signature
BIK	6.08	7.23	5.99	5.22	0.55	1.22E-11	AITL microenvironment signature
PGF	5.43	5.92	5.73	4.89	0.55	1.22E-11	AITL microenvironment signature
SCARA3	4.57	5.2	5.2	3.69	0.55	1.22E-11	AITL microenvironment signature
THY1	7.4	7.84	7.82	6.69	0.54	1.26E-11	AITL microenvironment signature
NT5DC4	5.25	6.23	5.71	3.76	0.54	1.93E-11	
FAM69A	7.79	7.95	7.51	7.04	0.54	2.23E-11	
OSMR	6.12	6.47	6.54	5.24	0.53	3.25E-11	AITL microenvironment signature
TMSB15A	5.29	5.9	6.33	4.22	0.52	1.27E-10	AITL microenvironment signature
FCAMR	4.27	5.22	5.44	3.01	0.52	1.69E-10	AITL microenvironment signature
GP1BA	6.8	7.11	6.88	6.06	0.52	1.86E-10	AITL microenvironment signature
LIF	6.36	6.75	6.46	5.03	0.52	1.98E-10	TNFA via NFKB Signaling; IL2 STAT5 Signaling; KRAS Signaling; AITL tumor signature
TUBB2B	5.46	5.79	5.7	4.12	0.52	1.98E-10	
EPAS1	9.71	10.08	10.21	9.14	0.52	1.98E-10	AITL microenvironment signature
ICOS	8.83	8.75	9.17	6.9	0.51	2.46E-10	IL2 STAT5 Signaling
CKAP2	9.91	10.69	10.23	7.97	0.51	2.46E-10	
ADAM19	8.37	8.53	8.45	7.41	0.51	2.92E-10	IL2 STAT5 Signaling; AITL microenvironment signature
FARP1	6.14	6.27	6.13	5.5	0.51	3.77E-10	
LY75	9.62	9.73	9.87	8.86	0.50	4.68E-10	
RSPO3	6.32	6.74	6.48	5.7	0.50	4.92E-10	AITL microenvironment signature
AFF3	6.65	6.76	7.82	5.3	0.50	8.12E-10	
TLCD1	5.05	5.45	5.44	4.68	0.50	8.43E-10	AITL microenvironment signature

* Values reported are log2 expression values of the mean per group

**Correlation coefficients calculated for nodal lymphomas of TFH origin compared to PTCL-NOS

Supplementary Table S4. Amplifications and deletions of loci with genes implicated in oncogenesis

		AITL (n=60)		Other TFH PTCL (n=15)		PTCL-NOS (n=27)		Correlation with GEP	
Gene	**Location**	**Amp**	**Del**	**Amp**	**Del**	**Amp**	**Del**	**Correlation with GEP (yes/no/le*)**	**mean fold change vs. cases without events**
DNMT3A	2p23.3	-	-	-	-	-	11%	le	-
REL	2p16.1	-	-	-	-	-	7%	no	-
DOCK10	2q36.2	-	-	-	-	-	7%	yes	-2.07
IL17RD	3p14.3	-	-	-	-	-	7%	le	-
PPP2R3A, IL20RB, STAG1	3q22.3	2%	-	-	-	-	-	le	-
TLR1/6/10, RHOH	4p14	-	-	-	-	-	7%	yes	-1.91
MYO10	5p15.1	-	-	-	6%	-	-	no	-
BBS9	7p14.3	-	2%	-	-	-	-	no	-
MYC	8q24.21	-	-	-	-	-	7%	no	-
CDKN2A/B	9p21	-	2%	-	12%	-	4%	no	-
TET1	10q21.3	-	3%	-	-	-	-	no	-
PTEN	10q23.31	-	3%	-	-	-	-	yes**	-1.60
FSCB	14q21.2	-	3%	-	-	-	-	le	-
TP53	17p13.1	-	-	-	-	-	11%	yes	-1.64
DNMT1	19p13.2	-	-	-	-	-	4%	no	-

*le = low gene expression ($\log_2 < 4.5$), regardless of copy number changes; **borderline low expression

Supplementary Figures

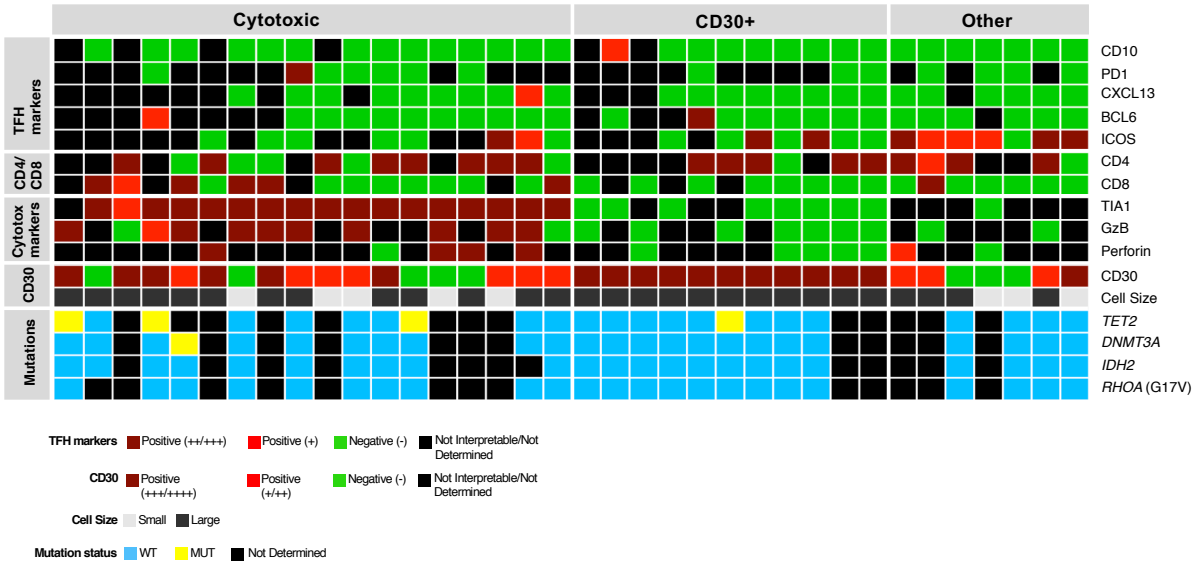

Supplementary Figure S1. Heatmap of cytological, immunophenotypical and mutational, features of 36 PTCL-NOS cases, comprised of 18 cytotoxic cases, 11 CD30+ cases with large cell morphology, and 7 cases ("Other") that do not fit either category and had expression of maximum one TFH marker (ICOS in most cases) out of 3 to 5 TFH markers tested. Note that the incidence of mutations in PTCL-NOS cases is low, in line with the description of the phenotype.

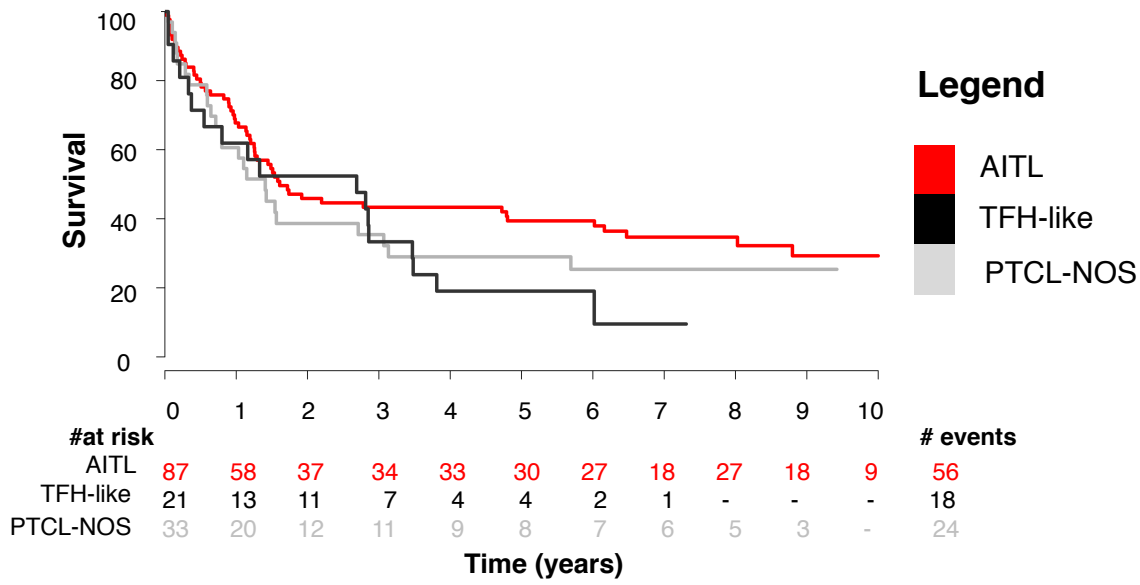

Supplementary Figure S2. No difference in the 10-year overall survival (OS) based on the Kaplan-Meier and log-rank methods is noted across the entities.

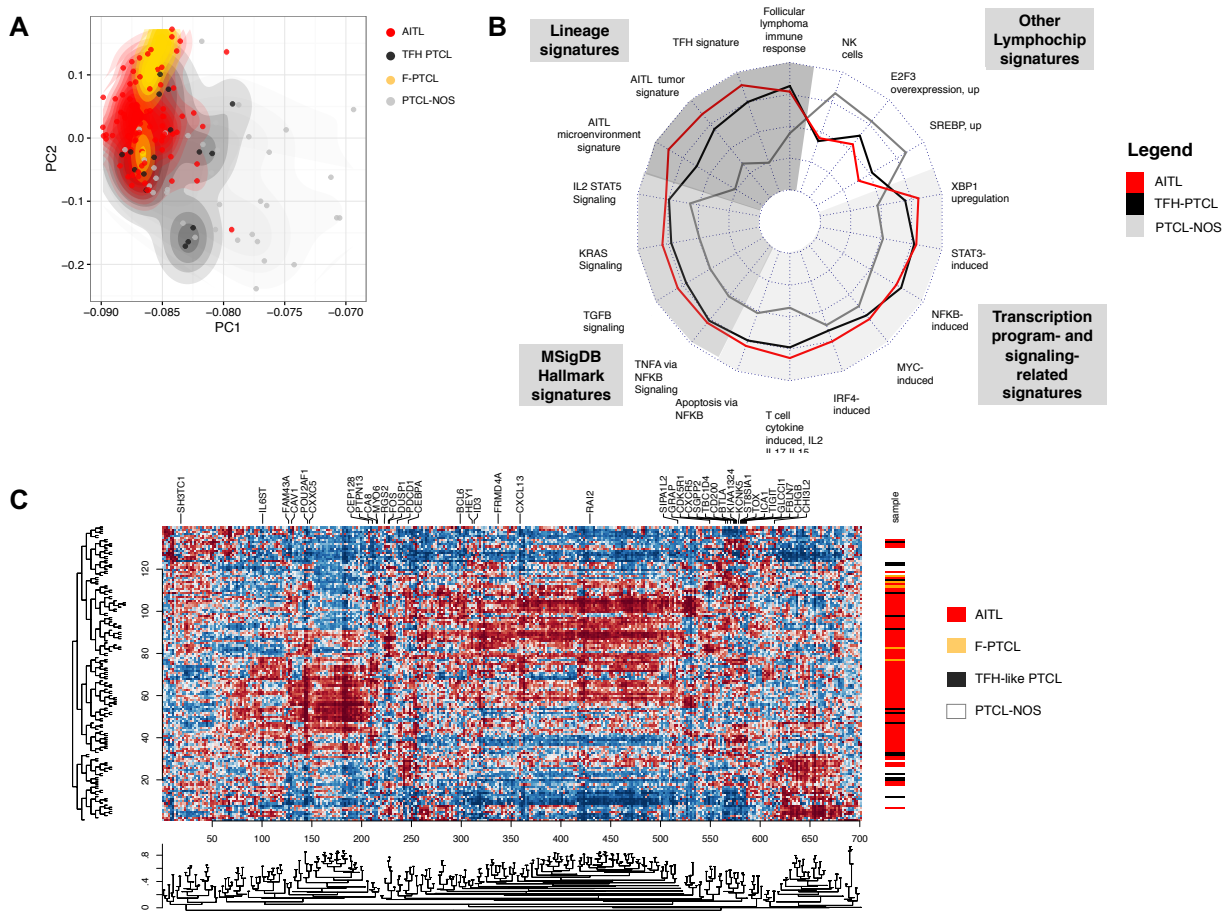

Supplementary Figure S3. 2D surface density plot of principal component analysis results **(A)**, featuring the first two principal components (PC1 and PC2, corresponding to a top view of the PCA in **Figure 1E**). Note the full inclusion of all F-PTCL in the volume occupied by AITL. Most PTCL of TFH origin (comprised of F-PTCL and other TFH PTCL; 14/20, 70%; contours of the volume occupied by TFH-like cases are indicated by dark grey lines), but not all, are also included within the volume occupied by AITL. The contour plot emphasizes the dispersion of the non-TFH-like PTCL-NOS. **(B)** Enrichment results for selected lineage-, hallmark and transcriptional program-related signatures further support the relatedness of PTCL of TFH origin to AITL. Enriched signatures include the IL2-STAT5, KRAS, TGFB and TNFA via NFKB signalling pathways, and downstream transcription factor targets of IRF4, MYC, STAT3 and NFKappaB. **(C)** Heatmap showing clustering of AITL, TFH-related and non-TFH-like PTCL, NOS based on the top 6000 most variable genes implicated in gene

set enrichments. Genes from the TFH signature are indicated on the columns. Majority of the PTCL of TFH origin (14/21, 67%), including all 5 F-PTCL, cluster with the main group of AITL cases.

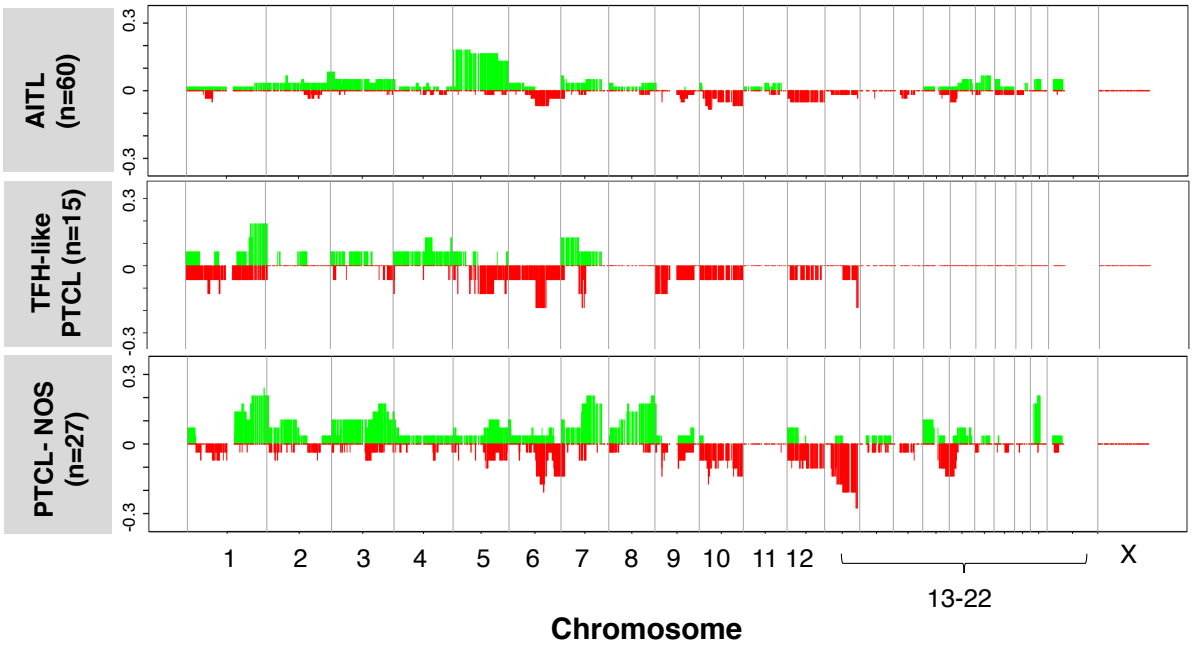

Supplementary Figure S4. Copy number events across categories show the proximity of the cytogenetic complexity of PTCL of TFH origin (mean event count per patient, MECP = 3.15) to AITL (MECP = 3.17) than to PTCL of TFH origin (MECP = 10.8). PTCL of TFH origin bear gains in chromosomes 5 and 7, which are characteristic aberrations in AITL.

References

1. de Leval L, Parrens M, Le Bras F, et al. Angioimmunoblastic T-cell lymphoma is the most common T-cell lymphoma in two distinct French information data sets. Haematologica. 2015;100(9):e361-4.
2. Bossard C, Dobay MP, Parrens M, et al. Immunohistochemistry as a valuable tool to assess CD30 expression in peripheral T-cell lymphomas: high correlation with mRNA levels. Blood. 2014;124(19):2983.
3. de Leval L, Parrens M, Le Bras F, et al. Angioimmunoblastic T-cell lymphoma is the most common lymphoma in two distinct French information data sets. Haematologica. 2015.
4. de Leval L, Rickman DS, Thielen C, et al. The gene expression profile of nodal peripheral T-cell lymphoma demonstrates a molecular link between angioimmunoblastic T-cell lymphoma (AITL) and follicular helper T (TFH) cells. Blood. 2007;109(11):4952-63.
5. Lemonnier F, Couronne L, Parrens M, et al. Recurrent TET2 mutations in peripheral T-cell lymphomas correlate with TFH-like features and adverse clinical parameters. Blood. 2012;120(7):1466-9.
6. Vallois D, Dobay MP, Morin RD, et al. Activating mutations in genes related to TCR signaling in angioimmunoblastic and other follicular helper T-cell-derived lymphomas. Blood. 2016;128(11):1490-502.
7. Monti S, Tamayo P, Mesirov J, Golub T. Consensus Clustering: A Resampling-Based Method for Class Discovery and Visualization of Gene Expression Microarray Data. Mach Learn. 2003;52(1-2):91-118.
8. Liberzon A, Subramanian A, Pinchback R, Thorvaldsdottir H, Tamayo P, Mesirov JP. Molecular signatures database (MSigDB) 3.0. Bioinformatics. 2011;27(12):1739-40.
9. Shaffer AL, Wright G, Yang L, et al. A library of gene expression signatures to illuminate normal and pathological lymphoid biology. Immunological reviews. 2006;210:67-85.
10. Chtanova T, Tangye SG, Newton R, et al. T follicular helper cells express a distinctive transcriptional profile, reflecting their role as non-Th1/Th2 effector cells that provide help for B cells. Journal of immunology. 2004;173(1):68-78.
11. Olshen AB, Venkatraman ES, Lucito R, Wigler M. Circular binary segmentation for the analysis of array-based DNA copy number data. Biostatistics. 2004;5(4):557-72.

Appendix

TENOMIC Consortium members: A. Martin, Hôpital Avicenne, Bobigny ; I. Soubeyran, P. Soubeyran, Institut Bergonié, Bordeaux; P. Dechelotte, A. Pilon, O.Tournilhac, CHU Estaing, Clermont Ferrand ; K. Leroy, P. Gaulard, MH Delfau, A Plonquet, C. Haïoun, F. Lebras, Hôpital Henri Mondor, Créteil; T. Petrella, L. Martin, JN Bastié, O Casasnovas, CHU, Dijon; B. Fabre, R. Gressin, D. Leroux, MC Jacob, M Calannan, CHU, Grenoble ; L. de Leval, D. Vallois, AL Roberti, A. Cairoli, CHUV, Lausanne, Suisse ; B. Bisig, G. Fillet, C. Bonnet, CHU Sart-Tilman, Liège ; M.C. Copin, B. Bouchindhomme, F. Morschhauser, CHU, Lille ; B. Petit, A. Jaccard, Hôpital Dupuytren, Limoges ; A. traverse-Glehen, E. Bachy, L. Genestier, B. Coiffier, CHU Sud, Lyon ; T. Rousset, P. Quittet, G. Cartron, Hôpital Gui de Chauliac-St Eloi, Montpellier ; B. Drenou, Hôpital E. Muller, Mulhouse ; K. Montagne, C. Bastien, S. Bologna, CHU de Brabois, Nancy ; C. Bossard, S. Le Gouill, Hôtel-Dieu, Nantes ; T. Molina, Hôtel-Dieu, Paris ; V. Meignin, J. Brière, C. Gisselbrecht, Hôpital St Louis, Paris ; B. Fabiani, S. Amorim, P. Coppo, Hôpital Saint-Antoine, Paris ; F. Charlotte, J. Gabarre, Hôpital Pitié-Salpétrière, Paris ; J. Bruneau, D. Canioni, V. Verkarre, E Macintyre, V. Asnafi, O. Hermine, R. Delarue, F Suarez, D. Sibon, JP Jaïs, Hôpital Necker, Paris ; M. Parrens, JP Merlio, K. Bouabdallah, Hôpital Haut Lévêque, Bordeaux ; F. LLamas-Gutierez, P. Tas, S. Maugendre-Caulet, T. Lamy, R. Houot, CHU Pontchaillou, Rennes ; JM Picquenot, L. Verezevan, P. Ruminy, F. Drieux, F. Jardin, C. Bastard, Centre H Becquerel, Rouen ; M. Peoc'h, J. Cornillon, CHU, Saint Etienne ; L. Lamant, C. Laurent, G. Laurent, L. Oberic, Hôpital Purpan, Toulouse ; J.Bosq, P. Dartigues, V. Ribrag, Institut G Roussy, Villejuif ; M. Patey, A. Delmer, Hôpital R. Debré, Reims ; JF Emile, K. Jondeau, Hôpital Ambroise Paré, Boulogne ; MC Rousselet, M. Hunault, CHU, Angers ; C. Badoual, Hôpital Européen Georges Pompidou, Paris ; C. Legendre,

F. Boidart, S. Castaigne, AL Taksin, CH Versailles, Le Chesnay ; J. Vadrot, A. Devidas, B. Joly, CH Sud francilien, Corbeil ; Dr Gandhi DAMAJ, CHU Amiens.

F Lemonnier, A Dupuy, N. Martin-Garcia, INSERM U955, Créteil ; P Dessen, G Meurice, Institut G Roussy, Villejuif ; M Delorenzi, E Missiaglia, P. Dobay, Swiss Institute of Bioinformatics, Lausanne, Switzerland ; F Radvanyi, E Chapeaublanc, Institut Curie, Paris ; P. Ferrier, S. Spicuglia, CIML, Marseille ; J. Soulier, Hôpital St Louis, Paris ; C Thibault, IGBMC, Illkirsch

The LYSA (the Lymphoma Study Association)

V Fataccioli, Project Manager, Hôpital H Mondor, Créteil

or, Créteil